CMS Physics Analysis Summary

Contact: cms-pag-conveners-exotica@cern.ch 2009/07/10

Search for heavy narrow $t\bar{t}$ resonances in muon-plus-jets final states with the CMS detector

The CMS Collaboration

Abstract

The first long physics run of LHC is expected to take place at a centre-of-mass energy of 10 TeV, and to go on until an integrated luminosity of 200 pb^{-1} has been collected. At these energies, many physics models beyond the Standard Model predict heavy new particles preferentially decaying to top pairs. Such new particles are searched for with the CMS detector in final states with jets and a muon as resonances in the top pair mass spectrum. New methods are presented for the selection and analysis of these events with two highly-boosted top quarks.

1 Introduction

The top quark, discovered in 1995 by both Tevatron experiments [1, 2], is the only Standard Model (SM) fermion with a mass of the order of the electroweak symmetry breaking (EWSB) scale. As such, it plays a special role in many EWSB theories beyond the Standard Model (BSM). In models with top condensation such as technicolor and topcolor, the role of the SM Higgs boson is filled by a $\mathrm{t\bar{t}}$ bound state [3]. These models predict additional heavy gauge bosons, which couple strongly to top quarks, *e.g.*, colour-singlet Z′ [4–6], colour octets, such as colorons [7] or axigluons [8]. In two-Higgs-doublet models [9], like the minimal supersymmetric extension of the Standard Model (MSSM), a Higgs boson may couple strongly to top quarks. The weakness of gravity compared to other forces has been addressed in the context of extra dimensions, such as the Rundall-Sundrum [10] and ADD models [11]. Here, TeV-scale gravitons can decay, in some cases preferentially, to top pairs [12]. In all these cases, the production of top pairs at hadron colliders through BSM mechanisms distorts the $\mathrm{t\bar{t}}$ invariant mass ($M_{\mathrm{t\bar{t}}}$) spectrum relative to the SM expectation, as described in Ref. [12].

The experimental sensitivity to a narrow resonance was studied in the $M_{\mathrm{t\bar{t}}}$ distribution in as model independent a way as possible. The goal is to show the exclusion potential for a narrow resonance topcolor Z′ [13] already studied at the Tevatron, with an integrated luminosity of $200\,\mathrm{pb}^{-1}$ expected to be collected in 2010 with the CMS detector [14] at a centre-of-mass energy ($\sqrt{s}$) of 10 TeV. This study focuses on the search for new heavy particles with a mass above $1\,\mathrm{TeV/c^2}$, and decaying into $\mathrm{t\bar{t}}$, where one of the top quarks decays hadronically ($\mathrm{t} \to \mathrm{Wb} \to \mathrm{q\bar{q}'b}$) and the other semi-leptonically ($\mathrm{t} \to \mathrm{Wb} \to \mu\nu\mathrm{b}$).

This note is structured as follows. Event generation and detector simulation is discussed in Section 2, followed by a discussion of event selection and analysis in Sections 3 and 4, respectively. The statistical analysis of the data is outlined in Section 5. Systematic uncertainties are discussed in Section 6.

2 Simulation

Standard Model $\mathrm{t\bar{t}}$ events are generated with the Monte Carlo event generator MADGRAPH/MADEVENT [15]. The subsequent parton showering of these quarks and gluons is described with PYTHIA [16]. Specifically, gluon and quark radiation off the $\mathrm{t\bar{t}}$ system is described with the QCD matrix element determined up to order α^3_{QCD}. In addition, MADGRAPH is used to produce generic high-mass resonances, via the implementation of a simple Z′ model with standard left- and right-handed couplings to fermions. In this implementation, the mass of the Z′ can be chosen freely and the width of the resonances is set arbitrarily to 1 % of the Z′ mass. This value is well below the experimental resolution, hence serves as generic model for narrow resonances. The parton showering is modeled with PYTHIA.

For the description of the non-top SM backgrounds the combination of MADGRAPH+PYTHIA as well as the generator PYTHIA alone are used. The former is used for the description of W and Z boson production in association with jets (W/Z+n jets, $n \leq 4$, W+$\mathrm{b\bar{b}}$/$\mathrm{c\bar{c}}$+n jets, $n \leq 2$). The latter is used for the description of generic multi-jet (QCD) processes. All simulations are performed at the centre-of-mass energy of 10 TeV, and make use of the CTEQ6L PDF parameterization [17]. All events are processed with a detailed detector simulation based on the GEANT4 toolkit [18] and reconstructed with the same reconstruction algorithms [14] foreseen for data.

3 Event Selection

The selection criteria presented in this section aim at retaining $t\bar{t}$ candidate events with two highly-boosted top quarks, the first decaying semi-leptonically into $b\mu\nu$, and the second hadronically. A similar study with both tops decaying hadronically is presented in Ref. [19]. The branching ratio of this muon+jets final state is about 15 %.

Only events accepted by a single-muon trigger, which requests a muon with p_T larger than 15 GeV/c and no isolation criteria, are selected. The trigger efficiency is determined to ranges between 85 % and 90 % for $Z' \to t\bar{t}$ with $M_{Z'}$ between 1 and 3 TeV/c^2.

At least one muon candidate [20] is required to be reconstructed within the muon detector acceptance ($|\eta| < 2.1$) with a p_T larger than 25 GeV/c and with a transverse impact parameter with respect to the beam spot smaller than 0.2 mm (as is expected from the prompt $W \to \mu\nu$ decay). If several muons satisfy these criteria, only the leading muon is considered for further analysis.

Jets are reconstructed using the SisCone algorithm [21] with a cone radius R in the (η,ϕ) plane of 0.5, using energy deposits measured in the calorimeters as input. Relative and absolute jet-energy corrections [22] are applied to account for the dependence of the jet response on η and p_T. In the following, jet p_T values always refer to this corrected value. Similarly, the missing transverse energy E_T^{miss} in the event is reconstructed using calorimetric information, and is corrected for jet-energy scale and for the presence of muons as described in Ref. [23].

At least two jets are required to be reconstructed in the tracker acceptance ($|\eta| < 2.4$) with a p_T larger than 50 GeV/c. The leading jet, possibly arising from the merging of the three quark jets from the hadronic top decay, is required to have a p_T in excess of 260 GeV/c.

No cut on the energy deposits in the calorimeters in a cone around the muon trajectory is applied, because the muon and the jet from the semileptonic top decay might overlap for energetic top quarks. In place of this cut, events with $\Delta R_{min} < 0.4$ and $p_T^{rel} < 35$ GeV/c are vetoed to strongly reduce the QCD multi-jet background, where ΔR_{min} indicates the minimum distance between the candidate muon and any reconstructed jet with $p_T > 30$ GeV/c and p_T^{rel} is the transverse momentum of the muon relative to the direction of the closest jet with $p_T > 30$ GeV/c. In the following, this cut is referred to as "2D cut". For further background suppression, the leptonic transverse energy H_T^{lep}, defined as the scalar sum of transverse energies of the leading muon and E_T^{miss}, is required to exceed 200 GeV. The cut on H_T^{lep} was chosen to maximize $S/\sqrt{B}$ where S and B are the numbers of signal and background events reconstructed in the Z′ mass peak (Section 4). The value of 200 GeV is a trade-off between the optimized values for different $M_{Z'}$. The cut efficiencies for the 2D cut and the H_T^{lep} cut are presented in Fig. 1. A 2D-cut scaling parameter value of t represents the 2D cut at $\Delta R_{min} = 0.4 \times t$ and $p_T^{rel} = 35 \times t$ GeV/c, such that the chosen cut is reproduced for $t = 1$. Table 1 shows the numbers of events expected after applying this event selection.

4 Analysis of the Event Kinematics

The semileptonically decaying top quark, t_ℓ, and the hadronically decaying top quark, t_h, are reconstructed as described below.

The decay products of t_ℓ are a muon, a neutrino and a b jet. The muon momentum is obtained from the global fit of the corresponding track [14]. The neutrino transverse momentum is given by the measured missing transverse energy, $\vec{E}_T^{miss}$. The neutrino longitudinal momentum is

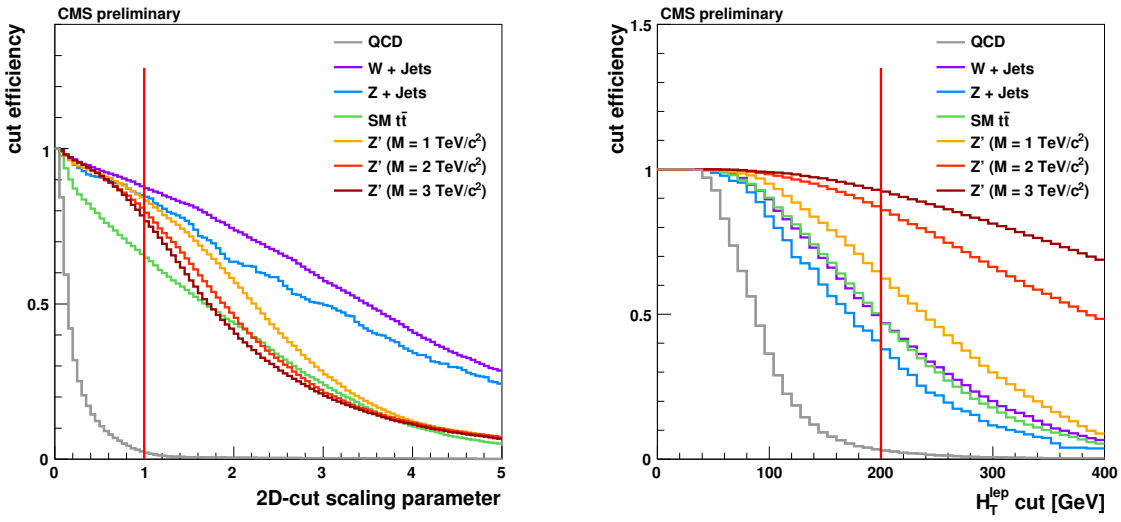

(a) (b)

Figure 1: Cut efficiencies for the cuts against QCD multi-jets and further backgrounds. The cut efficiencies are shown separately for different processes and the working value for each cut is indicated by a red line. Z′ only includes the decay to muon+jets. (a) 2D-cut scaling parameter (definition in the main text). (b) Efficiency for different $H_{\mathrm{T}}^{\mathrm{lep}}$ cut values, after applying the 2D cut.

Table 1: Expected event yield with an integrated luminosity of $200\,\mathrm{pb}^{-1}$ at $\sqrt{s} = 10\,\mathrm{TeV}$. The cross sections include branching ratios, corresponding to the decay channel indicated in the first column, if any.

Process	σ [pb]	N_{exp} in $200\,\mathrm{pb}^{-1}$
QCD multi-jet ($\hat{p}_{\mathrm{T}} > 50\,\mathrm{GeV/c}$)	280000 (LO)	7.3
$t\bar{t}$	414 (NLO+NLL)	127.0
W+jets ($\mathrm{W} \to \ell\nu,\ \ell = e, \mu, \tau$)	45600 (NLO)	159.5
Z+jets ($\mathrm{Z} \to \ell\ell,\ \ell = e, \mu, \tau$)	4200 (NLO)	10.4
single top (inclusive)	164 (NLO)	8.2
topcolor $\mathrm{Z}' \to \mathrm{t\bar{t}}$ (1 TeV/c^2)	3.28 (LO)	25.4
topcolor $\mathrm{Z}' \to \mathrm{t\bar{t}}$ (2 TeV/c^2)	0.13 (LO)	2.7
topcolor $\mathrm{Z}' \to \mathrm{t\bar{t}}$ (3 TeV/c^2)	0.01 (LO)	0.2

determined with a twofold ambiguity from the measured muon momentum and the known W mass. All real solutions (or the real parts of the solutions) of the corresponding quadratic equation are considered in the following. Each reconstructed jet can then be associated to either t_ℓ or t_h, or to neither of them. All possible combinations where at least one jet is associated to each of the top quarks are considered.

The chosen $(\mathrm{t}_\ell, \mathrm{t}_\mathrm{h})$ hypothesis is that which minimizes ΔR_{sum}:

$$\Delta R_{\mathrm{sum}} = \Delta R(\mathrm{t}_\ell, \mu) + \Delta R(\mathrm{t}_\ell, \nu) + \Delta R(\mathrm{t}_\ell, \mathrm{b}_\ell) - f_1 \Delta R(\mathrm{t}_\ell, \mathrm{t}_\mathrm{h}) - f_2 M_{\mathrm{t}_\ell \mathrm{t}_\mathrm{h}} \ , \tag{1}$$

where the various ΔR's indicate the distances in the (η, ϕ) plane between the leptonic top t_ℓ and the reconstructed muon μ, the reconstructed neutrino ν, the leading jet b_ℓ associated to t_ℓ, and the hadronic top t_h, respectively, and $M_{\mathrm{t}_\ell \mathrm{t}_\mathrm{h}}$ is the invariant mass of the reconstructed $\mathrm{t\bar{t}}$ system.

The first three terms of ΔR_{sum} account for the fact that a small separation of the decay products of the semileptonically decaying top quark is expected. The fourth term reflects the expectation of a large separation of the two tops in a resonant decay. The last term in Eq. 1 is included to reduce the tail towards low values of the reconstructed top pair mass. The resolution of the Z' peak as a function of f_2 and f_1 was studied and the values resulting in the best $M_{\mathrm{t\bar{t}}}$ resolution and the smallest tails are found to be $f_1 = 0.5$ and $f_2 = (0, 1, 5)/\mathrm{TeV/c^2}$ (for either 2, 3 or ≥ 4 jets, respectively). For illustration, a comparison between $M_{\mathrm{t\bar{t}}}$ distributions obtained with $f_2 = 0$ and $f_2 = 5/\mathrm{TeV/c^2}$ is displayed in Fig. 2a for $M_{Z'} = 2\,\mathrm{TeV/c^2}$. The resolution of the $M_{\mathrm{t\bar{t}}}$ reconstruction is displayed in Fig. 2b.

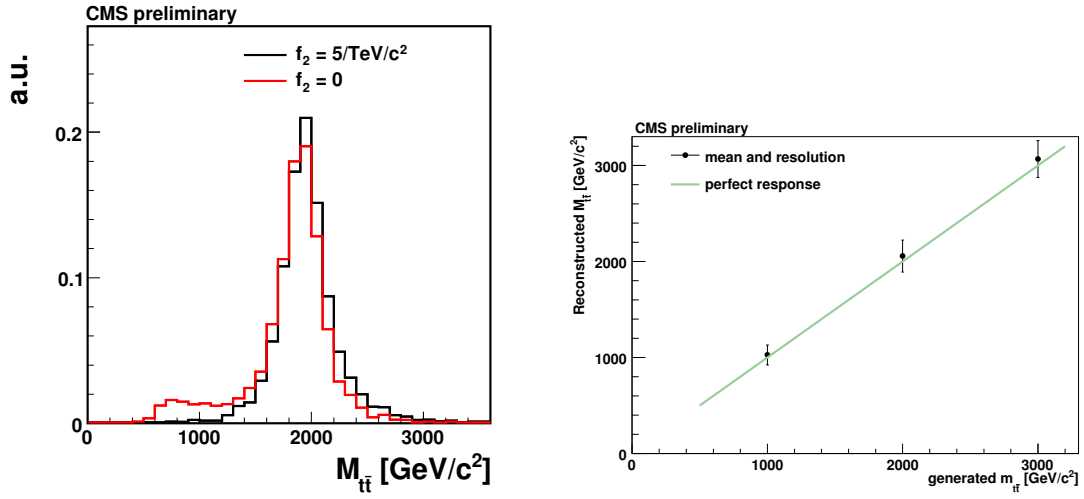

(a) (b)

Figure 2: (a) To illustrate the effect of f_2 in Eq. (1), $M_{\mathrm{t\bar{t}}}$ distributions obtained for $f_2 = 0$ and $f_2 = 5/\mathrm{TeV/c^2}$ are shown for $M_{Z'} = 2\,\mathrm{TeV/c^2}$. (b) The mean and width of the reconstructed $M_{\mathrm{t\bar{t}}}$ distribution versus the generated invariant mass of the $\mathrm{t\bar{t}}$ system.

5 Statistical Analysis

The extraction of the signal cross section, or of a 95 % C.L. upper limit on this cross section, is done by performing a fit of the $M_{\mathrm{t\bar{t}}}$ distribution, shown in Fig. 3a for the various backgrounds and various signal hypotheses. As this distribution cannot separate different background processes well, a simultaneous fit to data is performed in a sideband region and processes are constrained by using prior information for the cross section of the Standard Model $\mathrm{t\bar{t}}$ background process, for which an uncertainty of 20 % [24] was assumed.

This sideband region is defined by inverting the $H_{\mathrm{T}}^{\mathrm{lep}}$ cut with respect to the final selection, hence applying $H_{\mathrm{T}}^{\mathrm{lep}} < 200\,\mathrm{GeV}$. In this region, the QCD background process can be separated from the other backgrounds in the variable $H_{\mathrm{T}}^{\mathrm{lep}}$, as displayed in Fig. 3b.

The main backgrounds in the signal region are Standard Model $\mathrm{t\bar{t}}$ and W+jets (Table 1). As no missing transverse energy is expected, in general, for QCD multi-jet background, $H_{\mathrm{T}}^{\mathrm{lep}}$ is significantly lower for this background than for W+jets and $\mathrm{t\bar{t}}$. A fit of this distribution to the data therefore helps in determining the amount of QCD background. The W+jets and $\mathrm{t\bar{t}}$ backgrounds, however, cannot be disentangled by the $H_{\mathrm{T}}^{\mathrm{lep}}$ distribution. Only their overall

contribution can therefore be determined by this fit.

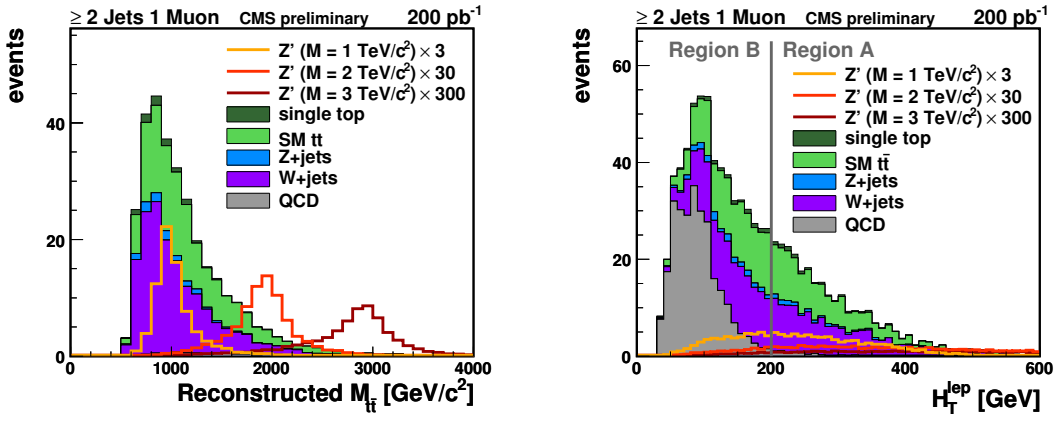

(a) (b)

Figure 3: Distributions of (a) $M_{\mathrm{t\bar{t}}}$ in Region A and (b) of $H_{\mathrm{T}}^{\mathrm{lep}}$ in Regions A and B, with superimposed Z′ signals. The Z′ cross sections used for this illustration purpose are given in multiples of the topcolor Z' cross section [13].

This background-enriched sideband is referred to as Region B. The signal region is called Region A. The rates of background events in Region A from QCD on the one hand, and from $\mathrm{t\bar{t}}$ and W+jets on the other, are determined from the rates obtained by the $H_{\mathrm{T}}^{\mathrm{lep}}$ distribution fit in Region B, and from the shape of the $H_{\mathrm{T}}^{\mathrm{lep}}$ distribution taken from the simulation in Region A+B.

Since the accuracy of the QCD multi-jet simulation might be insufficient to describe real QCD multi-jet data, the relevant distributions for QCD multi-jet events are obtained from another sideband highly enriched with QCD multi-jet events, called "QCD-shape sideband". This sideband contains only events rejected by the 2D cut, specifically events fulfilling $0.1 < \Delta R_{\mathrm{min}} < 0.4$ and $p_{\mathrm{T}}^{\mathrm{rel}} < 35\,\mathrm{GeV/c}$.

To model the $M_{\mathrm{t\bar{t}}}$ distribution for QCD multi-jet events in the signal Region A, all events from the QCD-shape sideband are used. To model the QCD multi-jet distribution in $H_{\mathrm{T}}^{\mathrm{lep}}$, the $H_{\mathrm{T}}^{\mathrm{lep}}$ cut is inverted in the QCD-shape sideband the same way as in the final selection, *i.e.*, the cut $H_{\mathrm{T}}^{\mathrm{lep}} > 200\,\mathrm{GeV}$ in the QCD-shape sideband is replaced by $H_{\mathrm{T}}^{\mathrm{lep}} < 200\,\mathrm{GeV}$.

The likelihood function of the simultaneous fit of the $M_{\mathrm{t\bar{t}}}$ and $H_{\mathrm{T}}^{\mathrm{lep}}$ distributions in Region A and B, respectively, depends on the cross sections of the signal and background processes. The package RooStatsCMS (RSC) [25] is used to make statistical inferences on the signal cross sections.

To determine the expected 95 % C.L. upper limit on the signal cross section, pseudo experiments without Z′ signal are generated. For each pseudo experiment, the likelihood function is calculated and used to construct confidence intervals based on likelihood ratio ordering in the large-sample limit [26].

To determine the value of $\sigma_{Z'}$ for which the $Z' \to \mathrm{t\bar{t}}$ production is expected to be observed with a 3σ and 5σ significance, respectively, pseudo experiments are generated for different input $\sigma_{Z'}$. A "background-only" model and a "signal-plus-background" model are fit to the data and the ratio of the likelihood values is calculated. A hypothesis test is performed at 3σ or 5σ where the null hypothesis is the validity of the "background-only" model. This test is done

by comparing the value obtained for this ratio to the expected distribution of this ratio for the "background-only" model. The probability to get an equal or better compatibility of this ratio with the "signal-plus-background" model is the desired significance.

6 Systematic Uncertainties

The following sources of systematic uncertainty are considered. The effects on the acceptance and on the shape of H_T^{lep} and $M_{t\bar{t}}$ are evaluated.

- It is assumed that for this early analysis, the jet energy scale (JES) will only be known to about 10%. All jet momenta are scaled by $\pm 10\%$, and E_T^{miss} is corrected accordingly.
- The uncertainty on the modelling of SM $t\bar{t}$ is estimated with PYTHIA samples generated with modified amounts of initial and final state radiation, obtained by varying the allowed parton virtuality in the shower and the evaluation of α_s in the shower. Additionally, MADGRAPH samples with varied factorization scale or varied thresholds for the matching of matrix element and parton shower contributions are used.
- The uncertainty on the modelling of W+jets is estimated with MADGRAPH samples, in which the factorization scale or thresholds for the matching of matrix element and parton shower contributions are varied.

While the acceptance uncertainty of the background processes can be as high as 60 %, the acceptance uncertainty on the signal is small in particular for the high-mass resonances. The uncertainty on the jet energy scale has the largest impact on the shape of $M_{t\bar{t}}$ and H_T^{lep} for both signal and background processes.

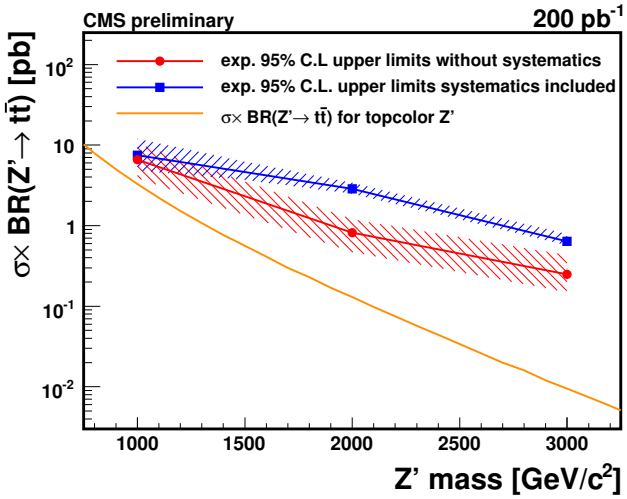

Figure 4: Expected limits (together with the 1σ confidence interval for these limits) on the Z' cross section at 95 % C.L. assuming an integrated luminosity of $200\,pb^{-1}$ collected with the CMS detector at $\sqrt{s} = 10\,TeV$, and the cross section of the topcolor Z' [13].

In order to deal with shape and rate systematics simultaneously, the convolution method used in many CDF analyses [27–32] was followed. Simulated samples with variations for systematic effects are used to measure the apparent shifts in the fitted $\sigma_{Z'}$ as a function of the true value. The sum of the shifts in quadrature is used as a width of a Gaussian resolution function

Table 2: Expected limits (together with the 1σ confidence interval for these limits) on the $\sigma_{Z'} \times \mathrm{BR}(Z' \to t\bar{t})$ at 95% C.L. assuming an integrated luminosity of $200\,\mathrm{pb}^{-1}$ collected with the CMS detector at a $\sqrt{s} = 10\,\mathrm{TeV}$. Limits obtained considering several sources of systematic uncertainties.

	Expected Limit [pb]		
considered uncertainties	$M_{Z'} = 1\,\mathrm{TeV/c^2}$	$M_{Z'} = 2\,\mathrm{TeV/c^2}$	$M_{Z'} = 3\,\mathrm{TeV/c^2}$
no systematic uncertainties	$6.6^{+3.8}_{-2.7}$	$0.8^{+0.4}_{-0.3}$	$0.25^{+0.18}_{-0.10}$
JES only	$7.4^{+4.4}_{-3.1}$	$2.8^{+0.6}_{-0.4}$	$0.60^{+0.14}_{-0.08}$
Q^2-scale only	$6.8^{+3.5}_{-2.1}$	$0.8^{+0.5}_{-0.3}$	$0.25^{+0.18}_{-0.13}$
threshold only	$7.0^{+2.7}_{-1.5}$	$1.0^{+0.4}_{-0.3}$	$0.26^{+0.15}_{-0.11}$
ISR/FSR only	$6.8^{+3.1}_{-2.0}$	$0.8^{+0.5}_{-0.3}$	$0.25^{+0.18}_{-0.10}$
all systematic uncertainties	$7.5^{+4.4}_{-2.7}$	$2.9^{+0.5}_{-0.4}$	$0.64^{+0.15}_{-0.07}$
predicted σ [pb] for topcolor Z′	3.28	0.13	0.01

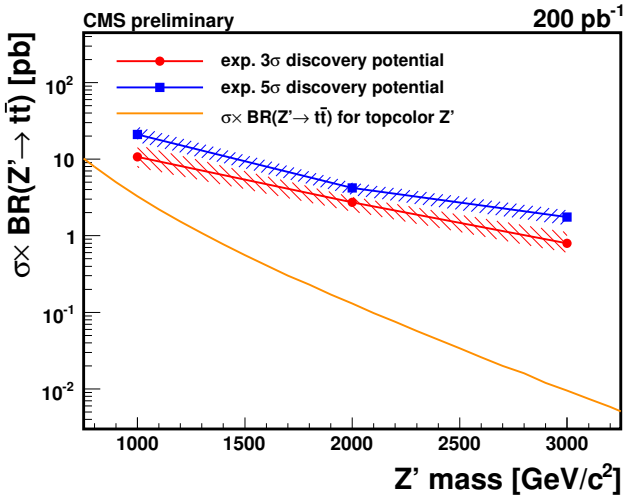

Figure 5: $\sigma_{Z'} \times \mathrm{BR}(Z' \to t\bar{t})$ (together with the 1σ confidence interval for this cross section) for which an observation of $Z' \to t\bar{t}$ production is expected at 3σ and 5σ, respectively, for an integrated luminosity of $200\,\mathrm{pb}^{-1}$ collected with the CMS detector at $\sqrt{s} = 10\,\mathrm{TeV}$, and the cross section of the topcolor Z′ [13].

that is folded with the likelihood, yielding a smeared likelihood function. The width of the Gaussian was parameterized as a linear function of $\sigma_{Z'}$. The upper limit including systematic uncertainties are then obtained in the same way as described above. In Fig. 4 and in Table 2, the expected 95 % C.L. upper limits without and with including all sources of uncertainty are shown as a function of $M_{Z'}$. The cross section expectation for a topcolor Z′ is also presented.

As cross check, two alternative fit models were studied. In the first, Standard Model $t\bar{t}$ is constrained to $\pm 100\%$ instead of $\pm 20\%$, and in the second, W+jets is constrained to $\pm 30\,\%$, while leaving $t\bar{t}$ free in the fit. The effect on the limits is only very small.

The lower values of $\sigma_{Z'} \times \mathrm{BR}(Z' \to t\bar{t})$, for which an observation of $Z' \to t\bar{t}$ production is expected with at least 3σ and 5σ, respectively, are shown in Fig. 5 and the cross sections including systematic uncertainties are presented in Table 3.

Table 3: $\sigma_{Z'} \times \mathrm{BR}(Z' \to t\bar{t})$ (together with the 1σ confidence interval for this cross section), for which an observation of $Z' \to t\bar{t}$ production is expected at 3σ and 5σ, respectively, for an integrated luminosity of $200\,\mathrm{pb}^{-1}$ collected with the CMS detector at $\sqrt{s} = 10\,\mathrm{TeV}$.

	Cross section for [pb]	
Z' mass [TeV/c^2]	3σ	5σ
1	$10.7^{+4.5}_{-2.9}$	$21.0^{+5.4}_{-4.3}$
2	$2.7^{+0.5}_{-0.6}$	$4.2^{+0.7}_{-0.8}$
3	$0.8^{+0.3}_{-0.2}$	$1.8^{+0.4}_{-0.4}$

Table 4: Median 95 % C.L. upper limits (together with the 1σ confidence interval for these limits), if using only $M_{t\bar{t}}$ in Region A for the likelihood function, *i.e.*, without the data in Region B, the low H_T^{lep} region. As comparison, the results for the method presented earlier which uses both regions is shown (cf. Table 2).

	Expected Limit [pb]	
Z' mass [TeV/c^2]	fitting $M_{t\bar{t}}$ only	fitting $M_{t\bar{t}}$ and H_T^{lep}
1	$9.8^{+10.6}_{-4.7}$	$7.5^{+4.4}_{-2.7}$
2	$3.8^{+2.1}_{-1.1}$	$2.9^{+0.5}_{-0.4}$
3	$1.1^{+0.5}_{-0.3}$	$0.6^{+0.2}_{-0.1}$

As a last cross check, limits were derived on the basis of a fit on the sole $M_{t\bar{t}}$ distribution to alleviate the reliance on the simulation for the H_T^{lep} extrapolation from Region B to Region A. The result of this check is shown in Table 4. While statistically less powerful, the sole use of the $M_{t\bar{t}}$ distribution is not affected by systematic uncertainties of the H_T^{lep} extrapolation, and lead to similar, albeit slightly worse, expected limits on the signal cross section.

7 Conclusion

An analysis was presented to search for narrow heavy resonances decaying to $t\bar{t}$ in the reconstructed top-pair mass spectrum in the muon+jets topology. This study focuses on the high top pair mass regime and complements another analysis in the muon+jets channel, which uses usual $t\bar{t}$ reconstruction techniques and has been designed to be optimal from production threshold up to 1–2 TeV/c^2 [33].

For an integrated luminosity of $200\,\mathrm{pb}^{-1}$ collected with the CMS detector at a centre-of-mass energy of 10 TeV the sensitivity to heavy narrow resonances was investigated. It was shown that the limits for this luminosity are at the level of a few picobarn or lower. While this is not sufficient to extend the currently excluded mass range for topcolor Z', $M_{Z'} < 820\,\mathrm{GeV/c^2}$ [34], limits for the investigated mass range 1–3 TeV/c^2 can be improved.

References

[1] **CDF** Collaboration, F. Abe et al., "Observation of top quark production in $\bar{p}p$ collisions," *Phys. Rev. Lett.* **74** (1995) 2626–2631.

[2] **DØ** Collaboration, S. Abachi et al., "Observation of the top quark," *Phys. Rev. Lett.* **74** (1995) 2632–2637.

[3] G. Cvetic, "Top quark condensation," *Rev. Mod. Phys.* **71** (1999) 513–574.

[4] J. L. Rosner, "Prominent decay modes of a leptophobic Z'," *Phys. Lett.* **B387** (1996) 113–117.

[5] K. R. Lynch, E. H. Simmons, M. Narain, and S. Mrenna, "Finding Z' bosons coupled preferentially to the third family at LEP and the Tevatron," *Phys. Rev.* **D63** (2001) 035006.

[6] M. S. Carena, A. Daleo, B. A. Dobrescu, and T. M. P. Tait, "Z' gauge bosons at the Tevatron," *Phys. Rev.* **D70** (2004) 093009.

[7] C. T. Hill and S. J. Parke, "Top production: Sensitivity to new physics," *Phys. Rev.* **D49** (1994) 4454–4462.

[8] P. H. Frampton and S. L. Glashow, "Chiral Color: An Alternative to the Standard Model," *Phys. Lett.* **B190** (1987) 157.

[9] D. Dicus, A. Stange, and S. Willenbrock, "Higgs decay to top quarks at hadron colliders," *Phys. Lett.* **B333** (1994) 126–131.

[10] L. Randall and R. Sundrum, "A large mass hierarchy from a small extra dimension," *Phys. Rev. Lett.* **83** (1999) 3370–3373.

[11] N. Arkani-Hamed, S. Dimopoulos, and G. R. Dvali, "The hierarchy problem and new dimensions at a millimeter," *Phys. Lett.* **B429** (1998) 263–272.

[12] R. Frederix and F. Maltoni, "Top pair invariant mass distribution: a window on new physics," *JHEP* **01** (2009) 047.

[13] R. M. Harris, C. T. Hill, and S. J. Parke, "Cross Section for Topcolor Z'_t decaying to $t\bar{t}$," `arXiv:hep-ph/9911288`.

[14] **CMS** Collaboration, G. L. Bayatian et al., "CMS physics: Technical design report,". CERN-LHCC-2006-001.

[15] F. Maltoni and T. Stelzer, "MadEvent: Automatic event generation with MadGraph," *JHEP* **02** (2003) 027.

[16] T. Sjostrand et al., "High-energy physics event generation with PYTHIA 6.1," *Comput. Phys. Commun.* **135** (2001) 238–259.

[17] J. Pumplin et al., "New generation of parton distributions with uncertainties from global QCD analysis," *JHEP* **07** (2002) 012.

[18] **GEANT 4** Collaboration, S. Agostinelli et al., "GEANT 4 – a simulation toolkit," *Nucl. Instrum. and Methods* **A506** (2006) 250–303.

[19] **CMS** Collaboration, "Search for High-Mass Resonances Decaying into Top-Antitop Pairs in the All-Hadronic Mode," *CMS PAS* **EXO-09-002** (2009).

[20] **CMS** Collaboration, "Measurement of the W and Z cross section with muons," *CMS PAS* **EWK-07-002** (2007).

[21] G. P. Salam and G. Soyez, "A Practical Seedless Infrared-Safe Cone jet algorithm," *JHEP* **05** (2007) 086.

[22] **CMS** Collaboration, "Plans for Jet Energy Corrections at CMS," *CMS PAS* **JME-07-002** (2008).

[23] **CMS** Collaboration, "$E_{\mathrm{T}}^{\mathrm{miss}}$ Performance in CMS," *CMS PAS* **JME-07-001** (2007).

[24] **CMS** Collaboration, "Early ttbar x-section in the muon+jets channel at 10 TeV," *CMS PAS* **TOP-09-003** (2009).

[25] D. Piparo, G. Schott, and G. Quast, "RooStatsCms: a tool for analyses modelling, combination and statistical studies," `arXiv:0812.2217`.

[26] W. A. Rolke, A. M. Lopez, and J. Conrad, "Confidence Intervals with Frequentist Treatment of Statistical and Systematic Uncertainties," *Nucl. Instrum. Meth.* **A551** (2005) 493–503.

[27] **CDF** Collaboration, T. Aaltonen et al., "Limits on the production of narrow $t\bar{t}$ resonances in $p\bar{p}$ collisions at $\sqrt{s}$ = 1.96-TeV," *Phys. Rev.* **D77** (2008) 051102.

[28] **CDF** Collaboration, A. A. Affolder et al., "Search for new particles decaying to $t\bar{t}$ in $p\bar{p}$ collisions at $\sqrt{s} = 1.8$ TeV," *Phys. Rev. Lett.* **85** (2000) 2062–2067.

[29] **CDF** Collaboration, D. E. Acosta et al., "Search for a W' boson decaying to a top and bottom quark pair in 1.8 TeV $p\bar{p}$ collisions," *Phys. Rev. Lett.* **90** (2003) 081802.

[30] **CDF** Collaboration, D. E. Acosta et al., "Search for single top quark production in $p\bar{p}$ collisions at $\sqrt{s} = 1.8$-TeV," *Phys. Rev.* **D65** (2002) 091102.

[31] **CDF** Collaboration, T. Aaltonen et al., "Search for resonant $t\bar{t}$ production in $p\bar{p}$ collisions at $\sqrt{s}$ = 1.96-TeV," *Phys. Rev. Lett.* **100** (2008) 231801.

[32] **CDF** Collaboration, D. E. Acosta et al., "Optimized search for single top quark production at the Fermilab Tevatron," *Phys. Rev.* **D69** (2004) 052003.

[33] **CMS** Collaboration, "Search for resonances close to top-pair production in the semileptonic muon channel at $\sqrt{s} = 10$ TeV," *CMS PAS* **TOP-09-009** (2009).

[34] **DØ** Collaboration, "Search for $t\bar{t}$ Resonances in the Lepton+Jets Final State in $p\bar{p}$ Collisions at $\sqrt{s} = 1.96$ TeV," *Conference Note* **5882-CONF** (2009).